

Investigation into the release of nanomaterials from can coatings into food

Johannes Bott^{a,b,*}, Angela Störmer^b, Peter Albers^c

^a Technical University of Munich, TUM School of Life Sciences Weihenstephan, Chair of Food Packaging Technology, Freising, Germany

^b Fraunhofer Institute for Process Engineering and Packaging (IVV), Freising, Germany

^c Evonik Technology & Infrastructure GmbH, Hanau, Wolfgang, Germany

ARTICLE INFO

Keywords:

Coatings
Nanomaterials
Migration

ABSTRACT

In this study internal and seam covering coatings as used in food cans were investigated on their potential to release nanomaterials (pigments, fillers) when food is stored and processed (sterilised) within coated cans. Two interior lacquers based on epoxy- and polyester- (with and without bisphenol A) resins and two seam covering coatings were used as lacquer matrices covering typical lacquer formulations. Eight different nanomaterials (four pigments and four fillers) were investigated that are typically used for adjusting colour and enhancing thermal and mechanical stability of the coatings. Aqueous sodium dodecylsulfate surfactant solution showed best suitability to disperse the nanomaterials with sufficient stability. A stable multi-nanomaterial dispersion, containing all eight nanomaterials at the same concentration each, was successfully used to develop an analytical method based on asymmetric flow filed-flow fractionation (AF4) coupled with multi angle laser light scattering (MALLS) detection and inductively coupled plasma mass spectrometry (ICP-MS) that allowed screening for possibly migrating nanomaterials at a limit of detection of 0.5 mg/dm². Coated metal plates were brought in contact with the aqueous surfactant solution as alternative food simulant for 2 h at 130 °C (sterilisation) followed by for 10 days at 60 °C (long-term storage). Via AF4/MALLS measurements the release of small oligomeric components from internal coating formulations was detected. However, the particle- and element-specific detection system demonstrated the none-migration of nanomaterials (fillers or pigments) from all test samples.

1. Introduction

Metal based packaging finds application as e.g. closures, lids, tubes, beverage and food cans. Metal food packaging benefits from its high thermal and mechanical stability. In case of canned food, metal based food packaging is the first choice due to its ability to keep the packaging undamaged and tight during sterilisation and long-term storage. Metal cans are produced from metal sheets (e.g. tin, aluminium, certain steel grades) that are usually rolled to cylinders and welded along the side wall (joint or seam). To prevent interactions between the metal and packed food (especially in case of e.g. acidic food) cans need to be lacquered or coated on the inside food contact side. The lacquer protects the metal from electrochemical reactions which may result in corrosion or gas formation (shaping) in the can. Furthermore the coating protects the food from release of metal ions which may cause sensory deterioration or even health related concerns (Oldring & Nehring, 2007). The metal sheets are coated by a liquid lacquer and heat cured before cutting and forming the cylinder or the end parts. After forming the base cylinder, there is a free metal edge at the seam which still needs to be protected. For this powder lacquers are used. In

the past mainly epoxy lacquers have been used for can coatings. Due to the critical discussion on Bisphenol A (BPA) which is a starting substance for the epoxy part, more and more alternative lacquers have been developed. An important group of these BPA non-intent lacquers is polyester based. In the lacquer formulation, additives are used to adjust properties of the coating like flexibility, mechanical/thermal stability, barrier effect or colour (Dubbart, Schwim, Völker, & Aper, 2014; Koleske, Springate, & Brezinski, 2013, Oldring & Nehring, 2007).

The special focus of this study is on pigments and fillers in the lacquers. Pigments are milled down to nanometer size in order to obtain fine dispersability. Others like carbon black or synthetic amorphous silica are produced ab initio as primary particles in the nanosize which are strongly fused together to aggregates and agglomerates (Flörke et al., 2012; Gray & Muranko, 2006; Wang, Gray, Reznick, Mahmud, & Kutsovsky, 2003). As fillers layered silicates are used which may exfoliate to platelets. These pigments and fillers are embraced by the definition of nanomaterials according to Commission Recommendation 2011/696/EU of the European Union (EU, 2011a, 2011b). Due to their high specific surface area, nanomaterials might be more reactive or have different physico-chemical properties than larger structured

* Corresponding author at: Technical University of Munich, TUM School of Life Sciences Weihenstephan, Chair of Food Packaging Technology, Freising, Germany.
E-mail address: johannes.bott@ivv.fraunhofer.de (J. Bott).

substances. But it is mostly unknown, whether nanomaterials exhibit a toxicological impact at oral exposure e.g. via food with the exception of synthetic amorphous silica (E551) and titanium dioxide (E171) which are used as direct food additives for decades. Due to this gap of knowledge the legislator acts precautious. In plastic materials for food contact, the risk of nanomaterials used as additives must be evaluated on a case-by-case basis. Only nanomaterials which are explicitly approved in their nano-form, are allowed to be used independently if in the direct food contact layer or behind a functional barrier (EU, 2011a, 2011b). Can coatings are not covered by the Plastics Regulation (EU) No. 10/2011 and there is not any specific regulation on the composition of such lacquers with exception of Commission Regulation (EC) No 1895/2005 on the restriction of use of certain epoxy derivatives in materials and articles intended to come into contact with food (EC, 2005). However, Article 3 of Commission Regulation (EC) No 1935/2004, which applies to any food contact material, requires:

“[...] any material or article intended to come into contact directly or indirectly with food must be sufficiently inert to preclude substances from being transferred to food in quantities large enough to endanger human health or to bring about an unacceptable change in the composition of the food or a deterioration in its organoleptic properties” (EC, 2004).

Risk is the product of hazard (toxicological properties) and exposure. Thus to evaluate the safety of nanomaterials used as additives in can coatings, a feasible way is to investigate whether exposure of the consumer to nanomaterials can occur, i.e. whether the nanomaterials are able to migrate out of the packaging (coating) into food. Within the last years a large number of studies investigating the migration of nanomaterials out of plastic materials into food or food simulants was published and also summarized in several reviews (Duncan & Pillai, 2015; Kuorwel, Cran, Orbell, Buddhadasa, & Bigger, 2015; Störmer, Bott, Kemmer, & Franz, 2017). However, until now the results are mostly not consistent and sometimes even contradictory. Investigating the migration potential of nanomaterials requires suitable analytical techniques and an experimental design that considers the particulate nature of the analyte throughout the experiment. The experimental design of many published migration studies did not allow exclusion of artefact formation and therefore the possibility of false-positive results (Addo Ntim, Thomas, & Noonan, 2016; Noonan, Whelton, Carlander, & Duncan, 2014; Störmer et al., 2017). The conclusion of this comprehensive comparison of the published studies was that nanoparticles which are completely embedded into a plastic polymer are immobilized in the polymer and will not migrate out of the polymer.

Studies on release of nanomaterials from lacquers on metal substrates like can coatings have not yet been published.

The scope of this study was to investigate whether those nanomaterials used as additives in can coatings will migrate into food. Thereby, the study comprised four different pigments, four different fillers and also different lacquers. This way, typical applications of internal as well as seam covering can coatings were considered. Combining asymmetric flow field-flow fractionation (AF4) with a multi angle laser light scattering (MALLS) detector and/or an inductively coupled plasma mass spectrometer (ICP-MS) allows for particle- and element-specific detection of nanomaterials in a suitable food simulant. The lacquers, especially the powder lacquers for seam covering, contained simultaneously several nanomaterials up to six nano-components. In total four pigments and four fillers, i.e. eight nanomaterials were investigated in the study. To handle this multitude of components, a multimethod was developed for simultaneous detection of the nanomaterials using a multi-nanomaterial dispersion as reference for calibration. The aim was to screen the food simulant taken from migration experiments for the presence of any of the respective nanomaterials.

Table 1
Description and composition of the four test-samples investigated in this study.

Application	Sample 1 interior lacquer	Sample 2 interior lacquer	Sample 3 Seam covering lacquer	Sample 4 seam covering lacquer
Lacquer-matrix	Epoxy	Polyester, BPA-n.i.a.	Polyester	Polyester
Film Thickness	200 µm	200 µm	120 µm	120 µm
Pigment	A	A	B	B + C + D
Filler	None	None	A + B + C	A + B + D

2. Materials and methods

2.1. Materials

Within the study four different can coatings (two interior and two seam covering coatings) were investigated which differed in the type of lacquer as well as in the number and amount of pigments and fillers used (Table 1). All can coatings were provided as flat tin plates lacquered with the respective coating formulation. The interior lacquers (provided by Schekolin AG, Liechtenstein) were applied onto laser-cut discs with $D = 116$ mm using a lab scale coating knife (sample 1 and 2, prepared and provided by Bruchsaler Farbenfabrik GmbH & Co. KG, Germany). For interior coatings two overlying layers of approx. 100 µm each were applied on the discs (total film thickness approx. 200 µm). It should be noted that usually in practice thinner coatings (typically 20 µm and less) are applied. However, coatings of more than 100 µm in thickness were used in this study to exclude formation of rust and to generate a worst-case in sense of higher a nanomaterial loading per test sample area. Seam covering powder lacquers (Schekolin AG, Liechtenstein) were lacquered as single layer of approx. 120 µm on tin plates in A4 format (sample 3 and 4, prepared and provided by Schekolin AG, Liechtenstein). Although the powder lacquers are usually applied as narrow bands on the seam only, full area coated plates were produced in order to enhance the sensitivity of the test. From sample 3 and 4 plates circular test specimens ($D = 116$ mm) were cut using tin snips. In total, the coated can samples contained eight different nanomaterials (four pigments and four fillers, Table 2) which were additionally provided as powders (Schekolin AG, Liechtenstein). The filler and pigment powders were used to produce reference dispersions for AF4/MALS and ICP-MS measurements. Reference samples without nanomaterials in the coating formulation were available for the interior lacquers sample 1 and sample 2 (Bruchsaler Farbenfabrik GmbH & Co. KG, Germany).

2.2. Preparation of nanomaterial reference dispersions

The scope of the dispersion experiments was to produce a stable multi-nanomaterial reference dispersion that contained all eight nanomaterials in the same concentration (“NM-mix”). An aqueous solution of ultrapure water (TKA Gen Pure, Thermo Scientific, USA) with each 2000 mg/l sodium hexametaphosphate (crystalline, Sigma Aldrich, USA), sodium dodecylsulfate (SDS, ultra-pure, Carl Roth, Germany) and polyvinylpyrrolidone (PVP, 1,3E6 g/mol, Alfa Aesar, USA) was used as dispersant for the preparation of individual stock dispersions first. 0.5 g of the respective nanomaterial were weighed out in 50 ml centrifugal vials and filled with 25 ml of the dispersant. All dispersions were treated with an ultra-sonication tip (Vibra Cell VC50T, Sonics & Materials, USA, 50 W, 20 kHz, 100% output) three times for 15 min successively to break up large agglomerates. During ultra-sonication the dispersions were cooled in an ice bath. At the end the dispersions were quantitatively transferred into 50 ml volumetric flasks, which were filled to the mark with the dispersant solution.

Dispersion prepared this way remained stable at room temperature without any optical change for 24 h. However, after approximately one

Table 2

Nanomaterials that were investigated in this study and that were used as pigments or fillers in the coating formulations.

	A	B	C	D
Pigment	“white” based on titanium dioxide ^a	“white” based on titanium dioxide ^a	“yellow” based on iron oxide	“black” based on carbon black (CB)
Filler	Kaolinite	Muscovite	Synthetic amorphous silica (SAS) – hydrophobic	Synthetic amorphous silica (SAS) – hydrophilic

^a Pigment A and B differ by the type of finishing.**Table 3**

Concentration of nanomaterials in the reference dispersions.

	Concentration “element” in nanomaterial-powder via XRF [%]	Concentration “element” in nanomaterial-dispersion (after centrifugation) via ICP-MS [mg/l]	Concentration “nanomaterial” in nanomaterial-dispersion (after centrifugation) [mg/l]
Dispersant Blank (Ti, Fe, Al)	/	< 0.05	/
Pigment A (Ti)	60.0	8.6	14.4
Pigment B (Ti)	58.2	3.1	5.3
Pigment C (Fe)	61.5	10.4	16.9
Filler A (Al)	21.0	9.7	46.4
Filler B (Al)	16.6	25.1	151.2
Pigment D (C)	/	/	10,000.0
Filler C (Si)	/	/	10,000.0
Filler D (Si)	/	/	10,000.0

week storage, the dispersions of pigments A–C as well as filler A and B showed sedimentation. Stable dispersions with known concentrations of the dispersed nanomaterial were essential for AF4 and calibration of the system. However, the supernatant of the mentioned dispersions still remained slightly cloudy and coloured. This indicated that the dispersions contained both, large agglomerates which remain only temporarily in the dispersion and have not been broken up to smaller units via ultra-sonication as well as smaller units that do not sediment. As the interest is on these smaller units in nanosize, the sediments and all unstable large agglomerates were removed by centrifuging the dispersions of pigments A–C as well as fillers A and B two times at 5000 G for 5 min. The smaller aggregates remained stable in the supernatant (indicated by a still apparent colour and opacity) which was transferred into new vials. To determine the amount of the nanomaterial in the supernatant, the content of the nanomaterial specific elements (Table 3) was quantified by ICP-MS and compared to the initial content of nanomaterial specific elements in the neat powders determined by X-ray fluorescence spectroscopy (methods described below). The dispersant itself did not contain detectable amounts of the nanomaterial specific elements. This way, the nanomaterial concentration in dispersion was found to be 14,4 mg/l (pigment A), 5,3 mg/l (pigment B), 16,9 mg/l (pigment C), 46,4 mg/l (filler A) and 151 mg/l (filler B). The dispersions of pigment D, filler C and filler D showed no sedimentation. Therefore the complete weighed portion was considered as fully dispersed corresponding to a concentration of 10.000 mg/l each. These stock dispersions were further diluted with the dispersant to a concentration of 100 mg/l.

This way sufficient stability of all dispersions and the concentrations of the dispersed nanomaterials were achieved. The diluted stock dispersions of the single nanomaterials were mixed together in a 100 ml volumetric flask to a stock dispersion that contained all nanomaterials at the same concentration simultaneously. After filling up the final NM-mix stock dispersion contained each nanomaterial at 1 mg/l (in sum 8 mg/l nanomaterial). Additionally, 3% acetic acid, the conventional food simulant B, was tested for the ability to produce stable dispersions. However, in 3% acetic acid the particles flocculated and sedimented rapidly. Therefore 3% acetic acid was not suitable for the study.

2.3. Transmission electron microscopy (TEM) with energy dispersive X-ray spectroscopy (EDX)

TEM images were prepared from the cross-section of lacquered samples to visualise the distribution of nanomaterials within the coating. Thereby, the border region between the can coating and the food contact side was of special interest, to see whether nanomaterials are fully embedded within the lacquer or stick out providing direct contact with food or food simulants.

Segments of the coated can samples were embedded within a synthetic resin and cut to ultrathin electron-translucent cryo-microtome sections. To enhance contrast of the images of the surface regions and to avoid artefacts caused by shear forces during cutting of the samples (e.g. shearing-off of particles, roughening of the lacquer surface) the topmost layers of the microtome sections microtomes were sputtered with a thin platinum/palladium (Pt/Pd) film.

Measurements were performed using a Hitachi H-7500 TEM operated at 100 kV acceleration voltage. EDX spot analysis was performed during TEM measurements to investigate the elemental composition of visualised particles using an Oxford EDX-detector and an INCA Energy 200 system.

2.4. Energy dispersive X-ray fluorescence spectrometry (XRF)

The spectrometer is able to measure powder samples directly. Therefore the powder was filled into a standard polypropylene cuvette. For this kind of sample preparation the cuvette is built of several parts using a PROLENE®-film of 4 µm thickness (Ethicon, USA). The filled sample was brought into the spectrometer chamber, which was rinsed by a continuous stream of helium. This way the absorption of fluorescence quanta by air components on the way to the detection system was minimized. The analysis was performed on an energy dispersive X-ray spectrometer (Spectro X-Lab2000, Spectro Analytical Instruments, Germany).

2.5. Inductively coupled plasma mass spectrometry (ICP-MS)

ICP-MS measurements were performed with the 7700 series ICP-MS (Agilent Technologies, USA) either in batch mode equipped with an ASX-520 autosampler (Agilent Technologies, USA) or coupled online

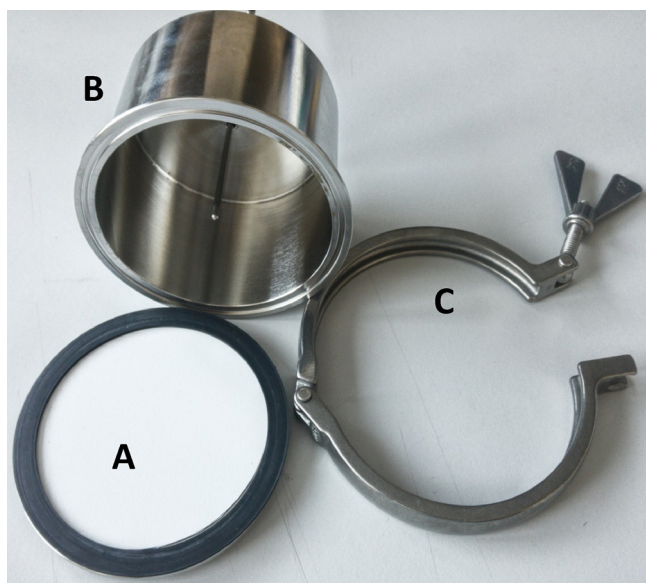


Fig. 1. Stainless steel migration cells: lid with test sample and EPDM-sealing (A), cell with food simulant and temperature sensor (B), lock ring (C).

with an asymmetrical flow field-flow fractionation (AF4) system. The ICP-MS was equipped with a micro mist nebulizer (Agilent Technologies, USA) and operated at 1550 W plasma power, 0,3 rps peristaltic pump speed and 151/min carrier gas flow rate (argon). By ICP-MS the amount of dispersed nanomaterial in the reference stock dispersions (batch mode) was quantified. Furthermore it was used as detection system of nanomaterial specific elements in simulants from the migration experiments (online mode). In online mode the ICP-MS was operated as described above but without using the peristaltic pump. The AF4 eluent was introduced into the ICP-MS via PN9050 Interface (Postnova Analytics, Germany). In batch mode Merck IV (1000 mg/l aluminium (Al) and iron (Fe)) and Merck XVII (100 mg/l titanium (Ti)) multi-element standard solutions (Merck Millipore, USA) were used to calibrate the ICP-MS on nanomaterial specific elements. For this the standards were diluted in 3% nitric acid to 50, 100, 200, 500, and 1000 ng/ml Al, Ti and Fe. The nanomaterial dispersions analysed in batch mode via ICP-MS were diluted by factor 50 with ultrapure water and then directly introduced in the ICP-MS via autosampler.

2.6. Asymmetrical flow field-flow fractionation (AF4)

AF4 measurements were carried out with the “AF2000 MT Series-mid temperature” (Postnova Analytics, Germany) system equipped with a 350 μm channel and a cellulose membrane (RC, cut-off: 10 kDa, Postnova Analytics, Germany). The channel was constantly maintained at 40 °C. A filtered 2000 mg/l SDS solution (0,1 μm Millipore filter disc) was used as flowing liquid for the AF4. The channel flows were controlled by “AF2000 Control Program” software (Postnova Analytics, Germany). Samples were injected into the channel at a flow rate of 0,2 ml/min with a focus flow rate of 1,0 ml/min. During the injection time of 30 min and an additional transition time of 0,5 min, the cross flow rate was kept constant at 0,5 ml/min. After transition (i.e. deletion of the focus flow, beginning of the elution phase) the cross flow rate was kept constant at 0,5 ml/min for additional 75 min with a detector flow rate of 0,5 ml/min. After the elution phase the channel was depleted by reducing the cross flow to 0,0 ml/min within 1,0 min and flushing the channel for 10 min at 0,5 ml/min detector flow rate. Samples were injected by full loop injections using a PNS300 series autosampler (Postnova Analytics, Germany) equipped with a 1000 μL sample loop.

2.7. Multi angle laser light scattering spectrometry (MALLS)

A 21-angle MALLS detector “PN3621” (Postnova Analytics, Germany) was used for the detection and characterization of particles, controlled by “AF2000 Control Program” software (Postnova Analytics, Germany). Sizes of the eluting particles were calculated as radius of gyration, r_g , using a random coil fit within the software. Sequential dilution of the NM-mix dispersion was used for concentration calibration of the MALLS detector, the determination of detection limit and particle size distribution. For this purpose, dispersions of 5, 10, 25, 50, 75 and 100 $\mu\text{g/l}$ NM-mix were prepared by diluting the NM-mix stock dispersion with a 2000 mg/l SDS-solution. Standard dispersions and a 2000 mg/l SDS-solution blank were prepared in triplicate and injected in duplicate in the AF4/MALLS system. The signal outputs of all MALLS angles were integrated with the analyser software Origin (OriginLab, USA) and combined to obtain the total peak area that was correlated to the concentrations of the sum of all eight nanomaterials in dispersion.

2.8. Migration tests

Migration was investigated using 2000 mg/l SDS solution as an alternative food simulant, due to its ability to keep the investigated nanomaterials in dispersion during migration testing. Coated metal plates (sample 1 to sample 4) were stored in stainless steel cells that allowed single sided contact of the coated side of the test samples with the simulant and avoided contact of the free metal cutting edges with the simulant. The test specimens in form of circular disks (116 mm diameter) were placed with the backside on the lid of the cell (i.e. upper part of the cell) which was then placed on the lower part of the cell containing the food simulant (see Fig. 1). The cell was sealed by an elastic ethylene propylene diene monomer (EPDM) ring with an inner diameter of 100 mm and an outer diameter of 120 mm. Thereby, the inner diameter of the sealing determined the contact area of the sample with the food simulant, which was 0,79 dm^2 . The cells (with test samples) were filled with 80 ml of 2000 mg/l SDS solution (stored at room temperature), firmly closed and stored at 130 °C in a temperature controlled oven. After the simulant within the cell reached the test temperature of 130 °C (after approx. 45 min) all cells were stored upside down for 2 h. Thereby, the temperature was controlled via temperature sensor inside the cell, see Fig. 1). After sterilisation, the cells were cooled under running water and then stored at 60 °C for additional 10 days. At end of storage time the migration solutions were transferred into glass vials and injected into the AF4/MALLS system directly (1000 μl injection volume). The migration experiments were carried out in triplicate and each dispersion was injected into the AF4/MALLS system twice. Cells filled with 80 ml surfactant solution only (sample blanks) were additionally prepared and stored under the same conditions as the test samples.

2.9. Stability testing under migration test conditions

To determine the stability of the nanomaterials in the NM-mix stock dispersion under migration test conditions 500 ml of 100 ng/ml NM-mix dispersion was freshly prepared. 80 ml of this dispersion were filled into the same migration test cells as used in the migration test and stored for 2 h at 130 °C and 10 d at 60 °C. Aliquots of the same dispersion were used as reference dispersions and measured by AF4/MALLS directly after preparation. The stability was determined as the ratio of the total peak areas of stored dispersions and freshly prepared dispersions. This ratio was used to calculate the detection limit of NM-mix dispersions under migration conditions. The stability test samples were prepared in triplicate.

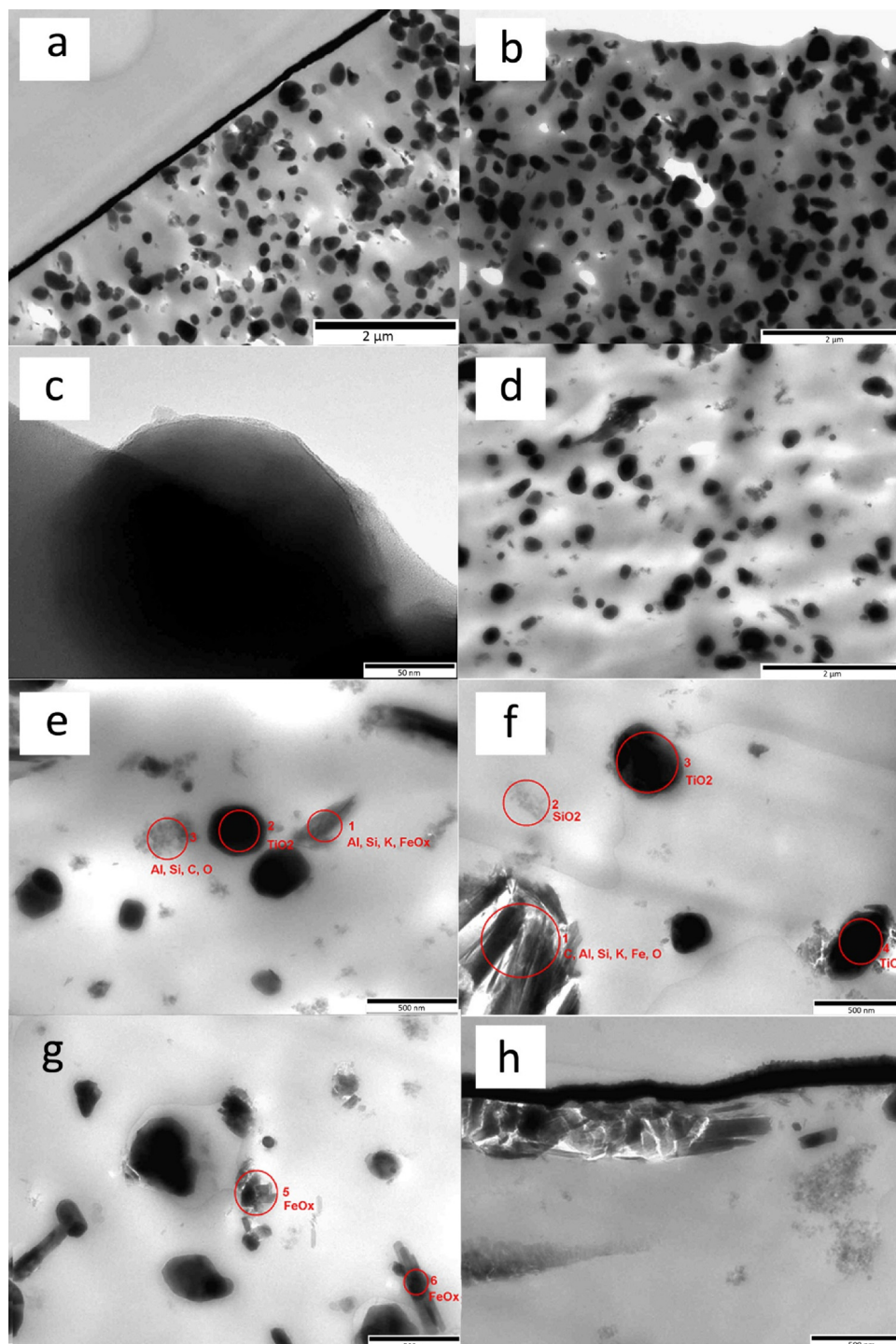


Fig. 2. TEM images of microtome sections of samples 1–4: sample 1 (a), sample 2 (b and c), sample 3 (d and e) and sample 4 (f–h). The red circles represent the individual sizes of the EDX-analysis spots.

3. Results and discussion

3.1. Characterisation of nanomaterials within the can coating by TEM/EDX

TEM images of sample 1 and 2 (Fig. 2a, b) showed that TiO_2 particles were homogeneously distributed within the lacquer coating. Thereby, TiO_2 particles exhibit compact structures of only few crystallites that are strongly fused together. Besides few square shaped structures TiO_2 particles predominantly showed compact spherical to ellipsoidal structures with sizes mainly of 100–400 nm in diameter.

However, somewhat smaller TiO_2 particles with diameters of less than 100 nm were found, too. Both TEM images clearly indicate that all particles are fully embedded within the lacquer matrix and do not stick out. However, in case of Fig. 2b it can be seen that the Pt/Pd sputter film was detached during the cryo-ultramicrotome cutting procedure, wherefore the border region between lacquer and food contact side becomes clearly visible. At this region only few particles were found that apparently seem to stick out of the lacquer, but at higher magnification (Fig. 2c) it could be visualised that a thin lacquer film was still surrounding the particle. TEM images of sample 3 (Fig. 2d, e) clearly

showed three different types of nanomaterials. Via the morphology obtained by TEM and the elemental composition as determined by nano-spot-EDX analyses a clear allocation of different nanomaterials was possible. Flat/linear expanded structures composed of Al, Si, FeO_x and K were typical for nanoclays (spot 1 in Fig. 2e), whilst spherical/ellipsoidal particles were identified as TiO₂ particles (spot 2 in Fig. 2e). The aciniform structure found (spot 3 in Fig. 2e) is usually typical for SAS, but the presence of other elements than Si and O indicated an aggregate of SAS and residues of clay. TiO₂ particles used in sample 3 (pigment B) showed the same morphology and size characteristics as the TiO₂ particles used in sample 1 and sample 2 (pigment A). Nanoclays found in sample 3 did not show agglomeration but also no exfoliation to single clay platelets, wherefore the predominant particle size and structure of clay were stacks with approximately 20–100 nm in thickness and lengths of approximately 200–500 nm. SAS was found to be present in form of aggregates with lengths/diameters of approximately 60–400 nm. Due to the variety of nanomaterials with different particle forms, sizes and micromechanical properties sample 4 presents a heterogeneous system when analysed by TEM. However, differences in elemental composition and morphology made differentiation between the different additives possible (Fig. 2f,g). TiO₂, SAS and clay particles/aggregates in sample 4 showed identical size and morphological characteristics than those nanomaterials found in sample 3. Additionally CB and iron oxide (FeO_x) were found as additives in sample 4. Whilst CB showed the same size and morphological (i.e. aciniform) characteristics as SAS, FeO_x particles showed square to rod-like structures. The smallest square-shaped structures showed edge lengths of 70 nm, whilst smallest rod-like structures had dimensions between 30 nm (thickness) and 500 nm (length). At the border region of some sample 4 coatings accumulation of clay structures as well as the presence of SAS aggregates was found (Fig. 2h). However, all nanomaterials were covered with lacquer and did not stick out of the coating layer.

In general, TEM/EDX allowed visualisation and identification of the nanomaterials used as additives in the lacquer formulations. Whilst most nanomaterials were homogeneously and finely dispersed within the coating, some clay aggregates were found to accumulate. However, all particles were fully embedded within the coating layer or in case of nanomaterials located at the border region between coating and food (simulant) fully covered with the lacquer. Uncoated nanomaterials at the surface of the coating were not found for in test sample.

As the dispersion experiments already indicated, TEM measurements showed a broad particle size distribution of nanomaterials used as pigments and fillers. TEM images of the coated can samples revealed that the smallest particle sizes of nanomaterials in the lacquer coating ranged from approximately 60–400 nm.

3.2. Characterisation of NM-mix dispersion by AF4/MALLS

Whilst the 2000 mg/l SDS solution blank caused no significant peak in the AF4 fractogram, injections of the NM-mix dispersion caused a pronounced void- and membrane release peak as well as a broad peak for the nanomaterials contained in the dispersion (Fig. 3). The signal at the beginning of the fractogram ($t = 30,5 \text{ min} - t = 40 \text{ min}$, “voidpeak”) and at the end of the fractogram (from $t = 106 \text{ min}$, “membrane release peak”) are typical for AF4 runs. The voidpeak elutes at the beginning of the AF4 run as soon as the sample is injected completely and the focus flow rate is deleted (approx. after 30,5 min). The membrane release peak elutes at the end of the AF4 run, after the separation force of the apparatus is eliminated in order to flush the separation channel. Both signals can be caused by the dispersant (e.g. residues of unbound PVP used in the stock dispersion), impurities in the samples and/or by large particles, that cannot be separated properly. Also changes in the system pressure, that appear after transition from injection to elution phase and after termination of the cross-flow, can cause those peaks. The nanomaterials themselves eluted during the elution phase from

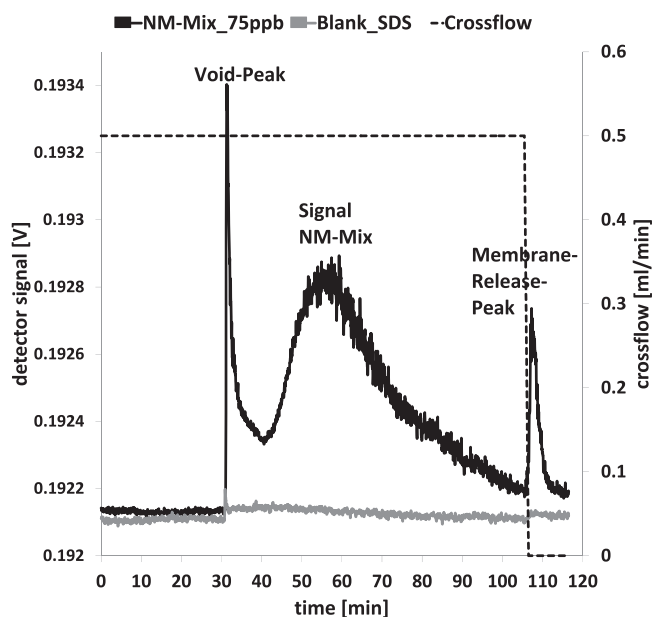


Fig. 3. AF4/MALS-fractograms of a NM-Mix dispersion (black; 75 ng/ml) and the dispersant blank (grey; 2000 mg/l aqueous SDS solution). Signals of the 92° detector. The dashed line is the progress of the cross-flow (separation force) during the AF4 run.

$t = 40 \text{ min}$ to $t = 106 \text{ min}$. The long elution time of more than one hour can be attributed to elution of nanomaterials with a broad particle size distribution during the elution phase with a constant separation force (cross flow) applied.

The evaluation of the MALLS signals resulted in a particle size distribution (mass weighted) from approx. $r_g = 70\text{--}600 \text{ nm}$, with 150 nm as the predominant particle size. Theoretically, r_g can be recalculated into a geometrical size (Andersson, Wittgren, & Wahlund, 2003). Under the assumption of a compact sphere, the calculated radii of gyration are corresponding to geometrical diameters (d_{geo}) of 90 nm–775 nm with 190 nm as the main particle size. However, geometrical diameters are only approximate values since the nanomaterials investigated in this study are no compact spheres but aggregated structures of fused primary particles or platelets in case of clay materials (filler A and filler B). The characterisation of the NM-mix dispersion revealed that a broad range of particle sizes is covered by the AF4 method. From the dispersion experiments it is known that the used pigments and fillers contain even larger aggregates/agglomerates, which had to be removed by centrifugation first. However, since migration is related to size dependent diffusion through the host matrix, especially smaller structures would have a higher potential to migrate, if any.

3.3. Detection limit and calibration of the AF4/MALLS system

NM-mix dispersions with nanomaterials concentrations in the range of 5, 10, 25, 50, 75 and 100 ng/ml (concentration of the sum of eight nanomaterials together in the respective dispersion) were used to calibrate the detector. Taking into account the angular dependence of the light scattering, the total peak area of all MALLS detector angles was calculated and plotted against the respective concentration (Fig. 4). The nanomaterial signal was found to be directly proportional to the concentration whereby the lowest detectable amount of nanomaterials was 5 ng at an injection volume of 1000 μL .

3.4. Stability of NM-mix structures at migration conditions

To ensure traceability of nanomaterials in food simulants taken from migration experiments sufficient stability of dispersed nanomaterials is essential. Dissolution of aggregates or sedimentation caused by

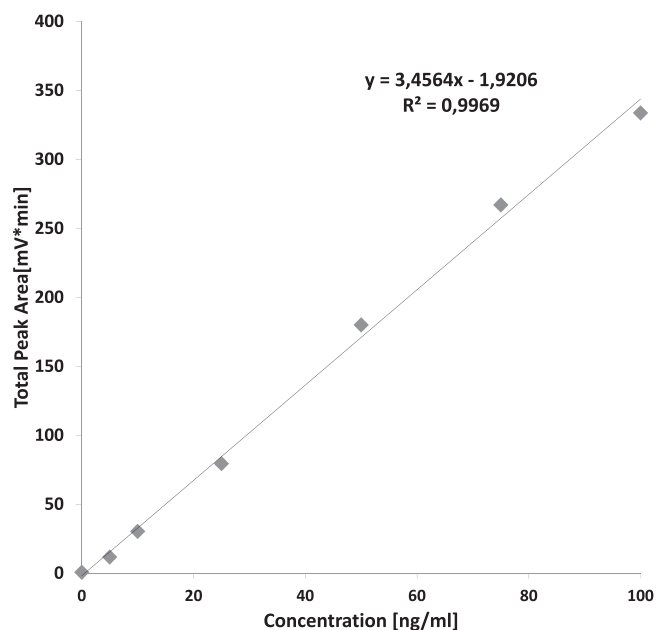


Fig. 4. Calibration function of NM-Mix dispersions derived by plotting the total peak area of AF4/MALLS signals versus the nominal concentration of the dispersions.

re-aggregation during storage of the migration samples might cause loss of the nanomaterial and thus false-negative results. Therefore, the influence of the storage in the 2000 mg/l SDS surfactant solution at test conditions on the stability of the dispersed nanomaterials was investigated.

After storage for 2 h at 130 °C and 10 d at 60 °C the total peak area of the AF4/MALLS signals were $95 \pm 4\%$ compared to the fresh dispersions (100 ng/ml NM-mix). Furthermore, with no shift in elution times it can be concluded that the nano-mix is stable. Neither re-aggregation nor dissolution of the nanomaterials was detectable which may influence the amount of dispersed particles as well as the particle size distribution.

Generally, the stability of dispersions depends on a variety of factors, like pH-value, ionic strength and the presence of stabilising additives (sterically and/or electrostatically stabilising agents) (Ruckenstein & Manciu 2010; Tadros, 2007). In this study the nanomaterials were dispersed by ultra-sonication in a dispersant that contained both, sterically (PVP) and electrostatically (SDS) stabilising agents. Via ultra-sonication large agglomerates were broken to smaller units, whereby the used surfactants prevented re-aggregation. The results of the stability testing showed that once the nanomaterial is dispersed, it remains stable even if only the 2000 mg/l SDS solution (without other additives) was used as dispersant for diluted dispersions and as flowing fluid for the AF4. This plays an important role in view of migration testing. The most suitable dispersant can be considered as the most suitable (alternative) food simulant. In conventional migration testing, the choice of the more severe food simulant is based on good solubility of the analyte in the simulant. In case of nanomaterials, a good dispersability of the nanomaterial assures fast transport of nanomaterial from the surface in the simulant and good capacity for the nanomaterial in the simulant which are the characteristics for a more severe simulant.

When nanomaterials are analysed, the particulate nature of the analyte has to be respected throughout the experiment. Dissolution of the nanomaterial in unsuitable food simulants might falsify the outcome of migration experiments when the nature of the migrating substance (i.e. ionic or particulate) has to be examined. This issue is especially a problem in case of metallic nanomaterials, like nanosilver, and was intensively reviewed recently (Störmer et al., 2017). In case of the investigated pigments and fillers, this problem of dissolution of the

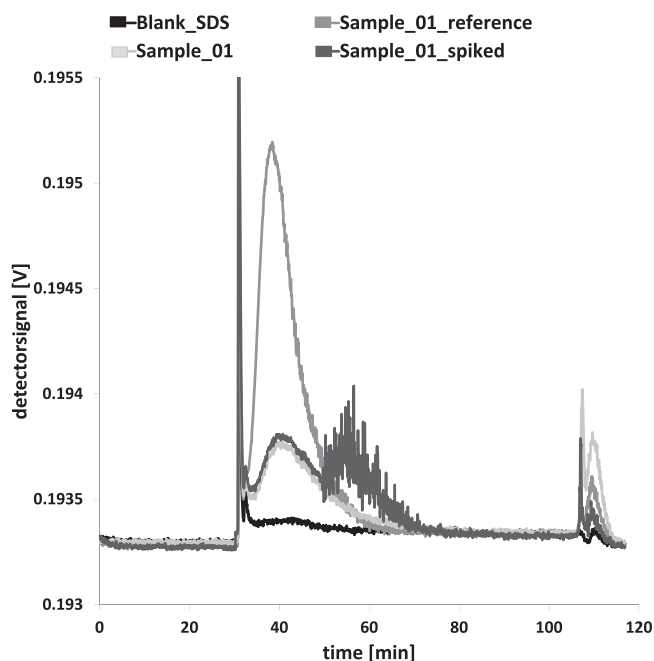


Fig. 5. AF4/MALLS fractograms of sample 1 migration experiments: 2000 mg/l SDS solution blank, test sample 1, test sample 1 additionally fortified to 10 ng/ml NM-mix, and the reference sample (from can coating without NMs).

particles obviously did not occur.

Due to the good stability of diluted NM-mix dispersions, the 2000 mg/l SDS solution is shown to be a suitable alternative food simulant for the nanomaterials in the study.

From the calculated stability rate of approx. 95%, the direct detection limit of the device of 5 ng (at 1000 μ l injection volume), the used amount of food simulant (80 ml) and the sample area of the can plates in contact with the simulant (0,79 dm^2) a surface related detection limit of 0,5 $\mu\text{g}/\text{dm}^2$ was calculated. Assuming a surface to volume ratio of 6 dm^2 per kg food, according to the EU cube model, the filling related detection limit corresponds to 3 μg NM-mix per kg food, whereby the NM-mix contained each nanomaterial (pigment A-D and filler A-D) at one-eighth.

3.5. Migration results

Injections of simulants taken from migration experiments of samples coated with the interior lacquer formulation (sample 1 and sample 2) caused only a peak at the beginning of the elution phase in the AF4/MALLS fractogram (sample 1: Fig. 5 and sample 2: Fig. 7) at elution time of from $t = 31$ –70 min. This peak partially interferes with elution times of the NM-mix ($t = 40$ –106 min). This peak was found in all replicates prepared from sample 1 and sample 2 specimens and also in the reference samples with the identical lacquers but without nano-additive (TiO_2 pigment). The peak did not appear in the simulant blank after storage under migration test conditions. In the reference samples the signals detected in AF4/MALLS runs were much more pronounced than those detected in the migration test samples with nanomaterials in the coating. Thus it can be concluded that under the applied migration test conditions the lacquer matrix itself released components into the food simulant. But after fortification of the food simulants from the migration experiment with the NM-mix dispersion to 10 ng/ml, the main part of the added nanomaterials eluted at the expected elution times but the signal was still superimposed by the signal starting at earlier elution times. The measurement of the NM-mix dispersion required low cross-flow rates wherefore the resolution of this method was limited. MALLS detection is non-specific and solely depending on the size of the analyte. In order to assure that the lacquer components peak does not hide

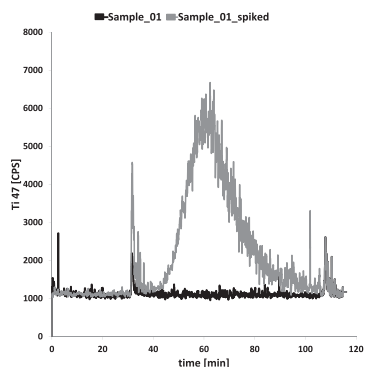


Fig. 6. AF4/ICP-MS measurements of sample 1 migration experiments. Signals for titanium of migration sample with a can coating containing TiO₂ based pigment A (black curve) and the same migration sample that was additionally fortified with the NM-mix dispersion to 10 ng/ml (1,25 ng/ml TiO₂) (grey curve).

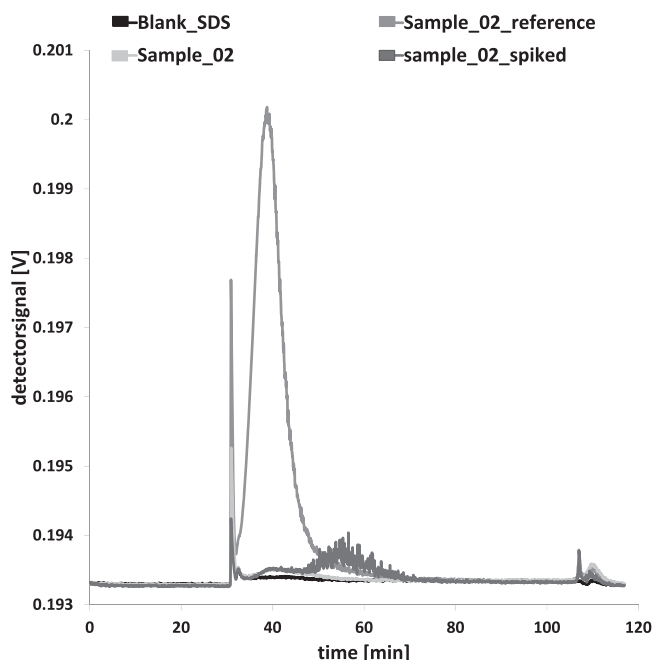


Fig. 7. AF4/MALLS fractograms of sample 2 migration experiments: 2000 mg/l SDS solution blank, test sample 2, test sample 2 additionally fortified to 10 ng/ml NM-mix, and the reference sample (from can coating without NMs).

migrating nanosized pigment fractions, the system was enhanced by online ICP-MS measurements for element-specific detection. Both samples (sample 1 and sample 2) contained TiO₂ based pigment (pigment A and pigment B) as the only nanomaterial in the coating formulation. Therefore, AF4 measurements on the same migration solutions from sample 1 and sample 2 were repeated with simultaneous detection of Ti via ICP-MS. AF4/ICP-MS fractograms of simulants taken from samples 1 and sample 2 migration samples (Fig. 6 and Fig. 8) showed no peak for titanium throughout the whole AF4 run. At elution times at which the lacquer matrix related peak was detected in the AF4/MALLS fractogram (t = 31–70 min), AF4/ICP-MS measurements demonstrated the absence of particles containing titanium. Also at elution times that were relevant for the TiO₂ particles (t = 40–106 min) no signal was detected. After fortification of the migration samples 1 and 2 with the NM-mix dispersion to 10 ng/ml (identical samples as used for AF4/MALLS measurements) a distinct peak for Ti at elution times t = 40–106 min was found without superimpositions of other matrix components. These fortification experiments demonstrated that the presence of other matrix components in the food simulants did not cause interferences in AF4/ICP-MS measurements and therefore do not

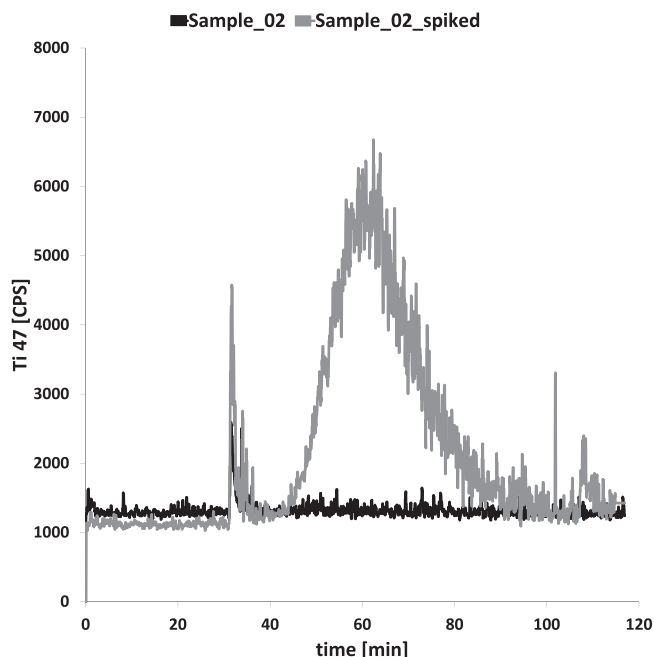


Fig. 8. AF4/ICP-MS measurements of sample 2 migration experiments. Signals for titanium of migration sample with a can coating containing TiO₂ based pigment B (black curve) and the same migration sample that was additionally fortified with the NM-mix dispersion to 10 ng/ml (1,25 ng/ml TiO₂) (grey curve).

affect detectability of TiO₂ particles in the food simulants. Thus, the presence of TiO₂ based pigment A and pigment B particles in the migration simulants from sample 1 and 2 can be excluded.

The lacquer related peak was caused by components that were extracted from the coating formulation of either samples, most probably oligomers or short polymer chains. Coatings based on epoxy- or polyester resins have been found to release oligomeric compounds (Ackerman, Noonan, Begley, & Mazzola, 2011; Biedermann & Grob, 1998; Grob, Spinner, Brunner, & Etter, 1999; Paseiro-Cerrato, MacMahon, Ridge, Noonan, & Begley, 2016; Paseiro-Cerrato, Noonan, & Begley, 2016; Schaefer, Mass, Simat, & Steinhart, 2004; Schaefer, Ohm, & Simat, 2004; Schaefer & Simat, 2004). AF4 with MALLS detects oligomers and polymer chains. An application of the technique is determining molecular weight distributions of polymers. AF4 signals of oligomers in migration solutions have also been observed in studies with plastic nanocomposites (Bott, Störmer, & Franz, 2014).

From samples coated with the seam covering lacquer (sample 3 and 4), in none of the migration simulants any peak was detected in the AF4/MALLS fractograms except for the system related void and membrane release peaks (Figs. 9 and 10). In contrast to samples coated with the interior lacquer formulation also no signals indicating a detectable

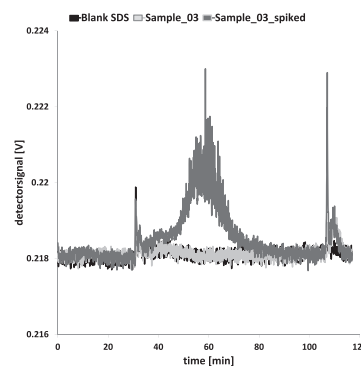


Fig. 9. AF4/MALLS fractograms of sample 3 migration experiments: 2000 mg/l SDS solution blank, test sample 3 and test sample 3 additionally fortified to 10 ng/ml NM-mix.

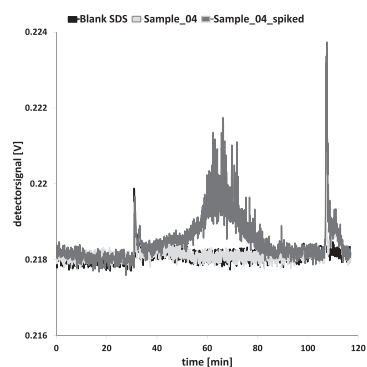


Fig. 10. AF4/MALLS fractograms of sample 4 migration experiments: 2000 mg/l SDS solution blank, test sample 4 and test sample 4 additionally fortified to 10 ng/ml NM-mix.

release of oligomeric lacquer components, was found. Fortification of migration simulants from sample 3 and 4 with the NM-mix dispersion to 10 ng/ml demonstrated that the nanomaterials could be recovered and detected by the system at the relevant elution times. Therefore, AF4/MALLS measurements demonstrated that no nanomaterials migrated into the food simulant.

From a phenomenological point of view the results in this study meet the expectation that nanomaterials are immobilized within a polymer matrix and do not migrate. Migration is a diffusion based process in which the migrant's size is the crucial parameter to determine the kinetic progress. With increasing size the free cross section of the migrant is enhanced leading to increased interactions with the surrounding polymer and less mobility of the migrant. The decreasing mobility of chemical substances in polyethylene terephthalate with increasing size was already demonstrated by Welle (Welle, 2013). In the recently published work of Franz and Welle (Franz & Welle, 2017) the migration potential of nano-spheres as worst-case material was modelled as a function of the particle size. In this study a “size-threshold” for migrating particles could be derived. Under the assumption of isolated, spherical particles and low density polyethylene (LDPE) as a host matrix with high diffusivity diffusion coefficients of $3,0 \cdot 10^{-9} \text{ cm}^2/\text{s}$ (1 nm particle), $5,4 \cdot 10^{-20} \text{ cm}^2/\text{s}$ (4 nm particle) and $4,4 \cdot 10^{-31} \text{ cm}^2/\text{s}$ (10 nm particle) were calculated, for example. The calculation of migration rates using these diffusion coefficients resulted only in relevant values when the nano spheres were small enough (1–3 nm). Already a sphere with 4 nm in diameter would cause migration in the lower ng/kg range (ppt), only. Migration from particles with larger diameters than that became negligible low. From these findings it is obvious, that nanomaterials intended as additive in food contact materials will be too large to migrate. Conventional nanomaterials do not exhibit isolated spherical particles but an aggregated structure of strongly fused particles. This typically yields in aggregate sizes that are by far too large to have a recognizable mobility within a polymer matrix. For example, in this study the measured particles sizes were in the range of 70–600 nm (calculated as radius of gyration). Thus, the theoretical considerations underpin the findings of the study that the nanomaterials are immobilized within the coating layer and do not migrate.

4. Conclusions

The scope of this study was to investigate whether pigments or fillers used in can coatings will migrate when in contact with food. The analytical method based on AF4/MALLS was capable to characterize and detect the eight nanomaterials in an aqueous surfactant solution used as alternative food simulant. The detection limit of 5 ng/ml for the mix of the nanomaterials corresponds to an area related detection limit of $0,5 \mu\text{g}/\text{dm}^2$ in the migration experiment.

The experimental design of the study and the used test conditions can be considered as very severe in sense of testing migration of

nanomaterials from cans into food. Both, the analytical techniques based on AF4/MALLS and AF4/ICP-MS as well as the use of a surfactant solution as alternative food simulant focused on unambiguous detection of migrating nanomaterials in their particulate form. The test condition 2 h at 130 °C followed by 10 d at 60 °C used in the migration study was chosen according to Plastics Regulation (EU) No. 10/2011. The 10 d at 60 °C simulate as accelerated test long-term storage of the packed food. Furthermore, sterilisation at 130 °C for 2 h can be considered as the most severe condition for sterilization, since usually lower time/temperature conditions (e.g. 30 min at 121 °C) are applied on packed food. Though the used conditions of the migration study can be considered as a worst-case in sense of migration of nanomaterials, the used nanomaterials did not migrate out of the lacquer into food. Like it has been shown for plastic materials, also in lacquers of can coatings nanomaterials are immobilized and do not migrate when fully embedded within the coating matrix.

Acknowledgements

The authors thank Dipl. Ing. (FH) Dominik Fiedler (Fraunhofer IVV Freising) for performing the XRF measurements of this study. The authors also wish to thank Mr. Christopher Kollera (Schekolin AG) for making available the lacquers/can coatings and Mr. Thomas Schleier (Bruchsaler Farbenfabrik GmbH & Co. KG) for his support in producing the flat tin plates.

References

- Ackerman, L. K., Noonan, G. O., Begley, T. H., & Mazzola, E. P. (2011). Accurate mass and nuclear magnetic resonance identification of bisphenolic can coating migrants and their interference with liquid chromatography/tandem mass spectrometric analysis of bisphenol A. *Rapid Communications in Mass Spectrometry*, 25, 1336–1342.
- Addo Ntim, S., Thomas, T. A., & Noonan, G. O. (2016). Influence of aqueous food simulants on potential nanoparticle detection in migration studies involving nano-enabled food-contact substances. *Food Additives & Contaminants*, 1–8.
- Andersson, M., Wittgren, B., & Wahlund, K.-G. (2003). Accuracy in multiangle light scattering measurements for molar mass and radius estimations. Model calculations and experiments. *Analytical Chemistry*, 75, 4279–4291.
- Biedermann, M., & Grob, K. (1998). Food contamination from epoxy resins and organosols used as can coatings: Analysis by gradient NPLC. *Food Additives & Contaminants*, 15, 609–618.
- Bott, J., Störmer, A., & Franz, R. (2014). Migration of nanoparticles from plastic packaging materials containing carbon black into foodstuffs. *Food Additives & Contaminants*, 31, 1769–1782.
- Dubbett, W., Schwirn Völker, K. D., & Aper, P. (2014). *Use of Nanomaterials in Coatings*. Germany: Fact Sheet – Federal Environment Agency.
- Duncan, T. V., & Pillai, K. (2015). Release of engineered nanomaterials from polymer nanocomposites: Diffusion, dissolution, and desorption. *ACS Applied Materials & Interfaces*, 7, 2–19.
- EC (2004). Regulation (EC) No 1935/2004 of the European Parliament and of the council of 27 October 2004 on materials and articles intended to come into contact with food and repealing Directives 80/590/EEC and 89/109/EEC. *Official Journal of the European Union*, L 338(4).
- EC (2005). Commission regulation (EC) No 1895/2005 of 18 November 2005 on the restriction of use of certain epoxy derivatives in materials and articles intended to come into contact with food. *Official Journal of the European Union*, L 302(28).
- EU (2011a). Commission recommendation of 18 October 2011 on the definition of nanomaterial (2011/696/EU). *Official Journal of the European Union*, 275, 38–40.
- EU (2011b). Commission regulation (EU) No 10/2011 of 14 January 2011 on plastic materials and articles intended to come into contact with food. *Official Journal of the European Union*, L 22(1).
- Flörke, O. W., Graetsch, H. A., Brunk, F., Benda, L., Paschen, S., Bergna, H. E., Roberts, W. O., Welsh, W. A., Libanati, C., Ettliger, M., Kerner, D., Maier, M., Meon, W., Schmolli, R., Gies, H., & Schiffmann, D. (2012). *Silica*. *Ullman's encyclopedia of industrial chemistry*. Weinheim: Wiley-VCH Verlag GmbH & Co. KGaA.
- Franz, R., & Welle, F. (2017). Mathematic modelling of migration of nanoparticles from food contact polymers. In R. Veraart (Ed.), *Nanosubstances in food contact materials; application, legislation and testing* DEStech Publications, Inc ISBN 978-1-60595-136-2.
- Gray, C. A., & Muranko, H. (2006). Studies of robustness of industrial aciniform aggregates and agglomerates—carbon black and amorphous silicas: A review amplified by new data. *Journal of Occupational and Environmental Medicine*, 48(12), 1279–1290.
- Grob, K., Spinner, C., Brunner, M., & Etter, R. (1999). The migration from the internal coatings of food cans; summary of the findings and call for more effective regulation of polymers in contact with food: A review. *Food Additives and Contaminants*, 16, 579–590.
- Koleske, J. V., Springate, R., & Brezinski, D. (2013). *Additives reference guide, paint and coatings industry magazine*. 6.

- Kuorwel, K. K., Cran, M. J., Orbell, J. D., Buddhadasa, S., & Bigger, S. W. (2015). Review of mechanical properties, migration, and potential applications in active food packaging systems containing nanoclays and nanosilver. *Comprehensive Reviews in Food Science and Food Safety*, *14*, 411–430.
- Noonan, G. O., Whelton, A. J., Carlander, D., & Duncan, T. V. (2014). Measurement methods to evaluate engineered nanomaterial release from food contact materials. *Comprehensive Reviews in Food Science and Food Safety*, *13*, 679–692.
- Paseiro-Cerrato, R., MacMahon, S., Ridge, C., Noonan, G. O., & Begley, T. H. (2016). Identification of unknown compounds from polyester cans coatings that may potentially migrate into food or food simulants. *Journal of Chromatography A*, 106–113.
- Paseiro-Cerrato, R., Noonan, G. O., & Begley, T. H. (2016). Evaluation of long-term migration testing from can coatings into food simulants: Polyester coatings. *Journal of Agricultural and Food Chemistry*, *64*, 2377–2385.
- Schaefer, A., & Simat, T. J. (2004). Migration from can coatings: Part 3. Synthesis, identification and quantification of migrating epoxy-based substances below 1000 Da. *Food Additives & Contaminants*, *21*, 390–405.
- Schaefer, A., Mass, S., Simat, T. J., & Steinhart, H. (2004). Migration from can coatings: Part 1. A size-exclusion chromatographic method for the simultaneous determination of overall migration and migrating substances below 1000 Da. *Food Additives & Contaminants*, *21*, 287–301.
- Schaefer, A., Ohm, V. A., & Simat, T. J. (2004). Migration from can coatings: Part 2. Identification and quantification of migrating cyclic oligoesters below 1000 Da. *Food Additives & Contaminants*, *21*, 377–389.
- Störmer, A., Bott, J., Kemmer, D., & Franz, R. (2017). Critical review of the migration potential of nanoparticles in food contact plastics. *Trends in Food Science & Technology*, *63*, 39–50.
- Wang, M.-J., Gray, C. A., Reznik, S. A., Mahmud, K., & Kutsovsky, Y. (2003). *Carbon black*. *Kirk-othmer encyclopedia of chemical technology*. John Wiley Sons, Inc.
- Welle, F. (2013). A new method for the prediction of diffusion coefficients in poly (ethylene terephthalate). *Journal of Applied Polymer Science*, 1845–1851.